Magnetotelluric data processing—a case study

J. M. Travassos* and D. Beamish
British Geological Survey, Murchison House, West Mains Road, Edinburgh EH9 3LA, *UK*

Travassos, J.M. & Beamish, D., 1988. Magnetotelluric data processing - a case study Geophysical Journal, 93, 377-391.

DOI: 10.1111/j.1365-246X.1988.tb02009.x

SUMMARY

Magnetotelluric (MT) data collected simultaneously at one or more sites may be processed by a number of different methods. Such methods attempt to remove or suppress the effect of noise on the data channels. The desired results are accurate, unbiased and repea estimates of the impedance tensor as a function of frequency and location. In this study we perform an investigation of the analysis of an MT data set sampled at 5 s. Both single-site (SS) and remote-reference (RR) techniques are employed to estimate the impedance tensor **Z**. Two biased SS estimates of **Z** are used to compare the performance of five coherence-based acceptance criteria. It is demonstrated that the RR predicted coherence between local fields can be used for selecting data windows, and provides a necessary assessment of the reliability of a given RR estimate. It is demonstrated that the variance of an RR estimate depends strongly on the local signal-to-noise ratios (as monitored by the local predicted coherence) and depends weakly on the number of data windows, as long as coherences are above a moderate threshold. Although, for our data, an estimate of **Z** obtained using a remote electric field is grossly inaccurate, its associated predicted coherence is as efficient in selecting low-noise-level data windows as its counterpart obtained using a remote magnetic field. The relation between SS and RR predicted coherences, the latter estimated using both electric and magnetic fields, is investigated. A hybrid selection technique that uses a remote electric field is suggested.

Key words: Data processing, electromagnetic induction, remote reference, single site

INTRODUCTION

MT data collected simultaneously at one or more sites may be processed using a variety of methods. The processing methods attempt to suppress or remove the effect of noise on the various data channels. The desired results of the processing should be accurate, unbiased and therefore repeatable determinations of the impedance elements as a function of frequency and location. This study takes typical MT field data and considers the effect of a number of processing methods on the impedance elements.

The MT data used here were sampled at 5 s for 7 days at two sites. The sites, here designated 1 and 2, straddle the North Anatolian Fault in Western Turkey. Fig. 1 shows the location of the two sites. Data were, in fact, collected over a six-month period as part of the Turkish Dilatancy Project (TDP3) of 1984 (Beamish & Riddick 1985a). The crust in this region is undergoing active dislocation as evidenced by an earthquake swarm within the survey area (Fig. 1). Subsets of the data are being used to provide EM response functions as a function of time for comparison with other geophysical parameters. The sampling period and the subset data length used for this case study can be considered 'typical' of long-period magnetotelluric collection schemes.

Conventional single-site MT processing uses only data channels recorded at a single site. Data collected simultaneously at two or more sites enables additional (remote) channels to be introduced into the analysis. Our test data set permits single-site and remote-reference processing methods to be compared. This study examines the procedures that can be used to obtain an accurate impedance solution at a particular location (site 2) given a typical simultaneous data set at two sites. The data obtained at site 1, located 29 km from site 2, are used for channel-referencing purposes.

MT data processing is straightforward when no noise exists. A large number of processing methods have been considered when noise is present (Sims *et al.* 1971; Gundel 1977; Goubau *et al.* 1978a,b; Larsen 1980; Park & Chave 1984). Here we adopt a simple processing strategy. We know that successive accumulations of data windows will contain varying amounts of signal, since we are dealing with *natural* source fields over a seven day interval. Superimposed on this natural signal variation are noise sources which can provide intense variations in the signal-to-noise (S/N) ratio. We therefore make the assumption that not all the accumulated data windows should contribute to the impedance solutions formed by the auto and cross-spectra of

* Permanent address: Departmento de Geofisica, CNPq—Observatorio Nacional, R. Gen. Bruce 586, 20921 Rio de Janeiro, RJ, Brazil.

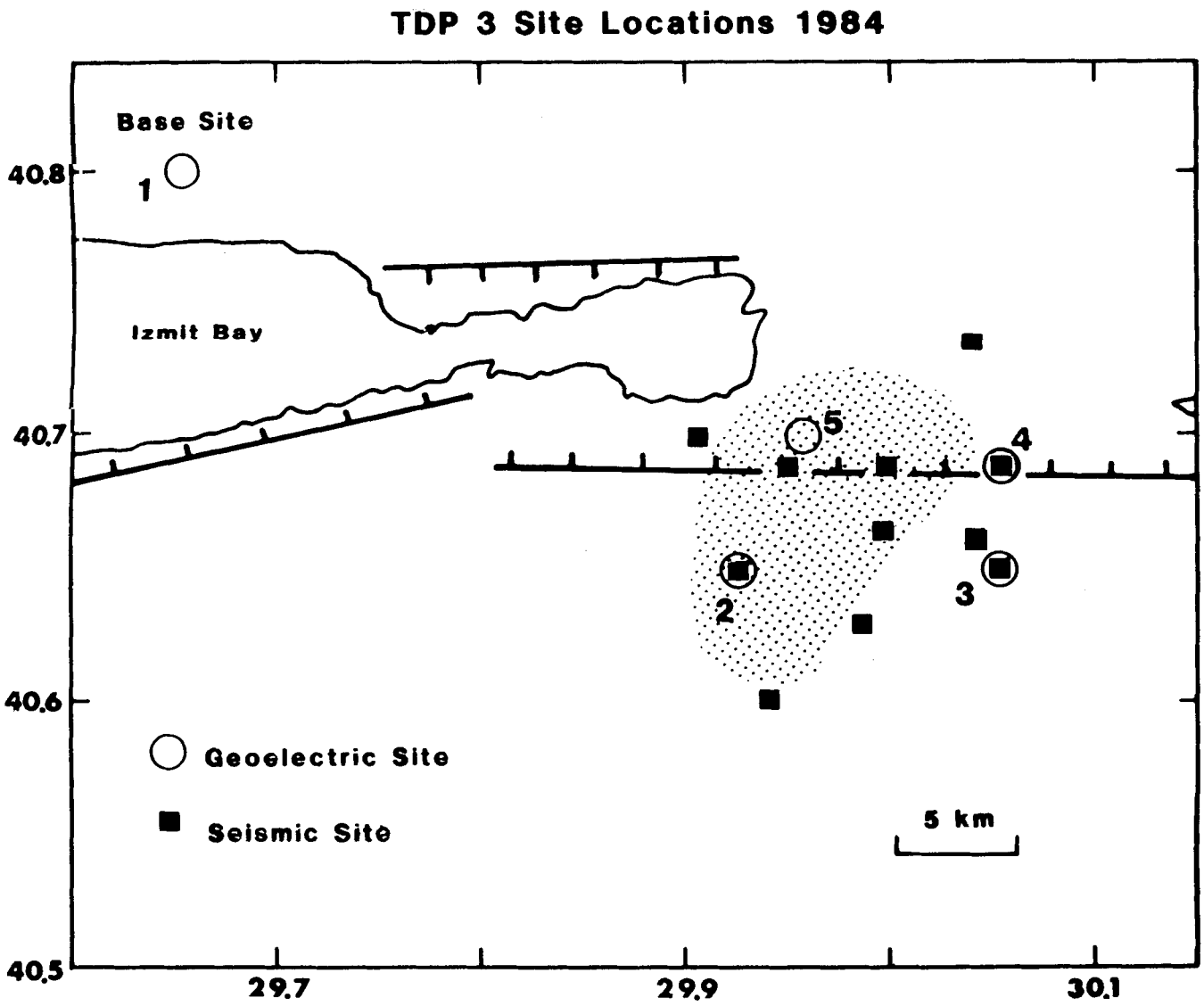

Figure 1. Site locations within the TDP3 area. The shaded area shows the location of a recurrent earthquake swarm. Sites labelled 1 and 2 are used in the present study with site 1 used as a reference. Fault margins are indicated by lines with cross-bars. Coordinates are geographic.

a particular window. The variation in the S/N quality of a given window is monitored by one or more coherence functions associated with a solution. If the S/N quality of a given solution is considered acceptable, then the spectra associated with the data window are stacked; if this quality is considered unacceptable the spectra are rejected. Weighting of the spectra is therefore performed in its most severe form: we use weights of 1 or 0 depending on whether a particular data window is accepted or not. Particular solutions for each frequency estimate are treated separately.

In the SS case, the data provide no information on the noise contribution from individual data channels. For this case we seek accurate bounds on the impedance function. The bounds are provided by biased solutions. The data from the local site are used to examine the behaviour of the solutions obtained from five different quality-tests. The tests are based on the coherence functions estimated with the local fields.

The introduction of additional reference channels enables the remote reference solutions (Gamble *et al.* 1979a) to be estimated. Although it has been suggested that this technique alleviates the need for spectral selection, we here retain and examine a coherence-based selection strategy. The reliability and, in particular, the accuracy of the impedance estimates is investigated using the solutions obtained with the magnetic reference channels. Results are compared with the equivalent estimates that can be obtained using the remote electric fields.

A comparison of S/N determinations using SS- and RR-derived coherence functions reveals that the SS-derived functions are often 'inadequate'. By retaining the selection role of coherence functions obtained from a remote reference analysis it is possible to achieve an adequate selection of data subsets using either magnetic or electric reference channels. Such a 'robust' selection enables a hybrid analysis scheme to be adopted for more limited data-collection schemes.

DATA ACQUISITION

The study area of the TDP3 experiment is shown in Fig. 1. A full description of the project is given by Evans *et al.*

(1987). There are four magnetotelluric sites within or close to an earthquake swarm, shaded in the figure. Site 1 is a base site to which all other sites were radio-linked. Only data sets from site 2 and site 1 are analysed. These two sites are situated 29 km apart on either side of the fault graben. Tri-axial fluxgate magnetometers were used to record the three magnetic components. Four electrodes were laid in a cross arrangement with 100 m distance between pairs. A fifth electrode provided a common ground. Electrodes were non-polarizing copper–copper sulphate designed for the TDP3 project. The sensors were aligned along the N–S, E–W magnetic directions. All data were low-pass filtered and amplified before conversion to digital form. All sites were radio-linked to site 1 by digital telemetry, the incoming signals being demodulated at the base. Data were collected using a minicomputer system. A detailed description of the system can be found elsewhere (Beamish & Riddick 1985b).

Data were sampled at 5 s during the six months of the TDP3 experiment. Five components were recorded at each site: *Ex, Ey, Hx, Hy* and *Hz*. The vertical magnetic component is not considered in the present study. Fig. 2 shows 1 hr of simultaneous measurements at both sites. Note that the natural scales of the electric components at site 1 are more than 13 times the corresponding components at site 2.

For spectral estimation purposes the data have been divided into two decades which are referred to as decades 4 and 5. The basic (raw) data series, sampled at $\Delta t = 5$ s, form decade 4 (10–100 s). A data window consists of 192 points, i.e. it has a length of 960 s. The seven days provide 630 such data windows. Each window provides sufficient degrees of freedom for spectral estimation of the MT response functions across a decade. The data set for decade 5 (100–1000 s) is produced by applying a low-pass filter to the basic data set and re-sampling at 50 s. Again a data window consists of 192 points, having a length of 160 min. The same seven days now provide 63 such data windows. It is important to point out that the data analysis scheme adopted here uses non-overlapping, i.e. independent, data windows. For each window, spectral band averaging using FFT provides 10 non-overlapping frequency bands per decade.

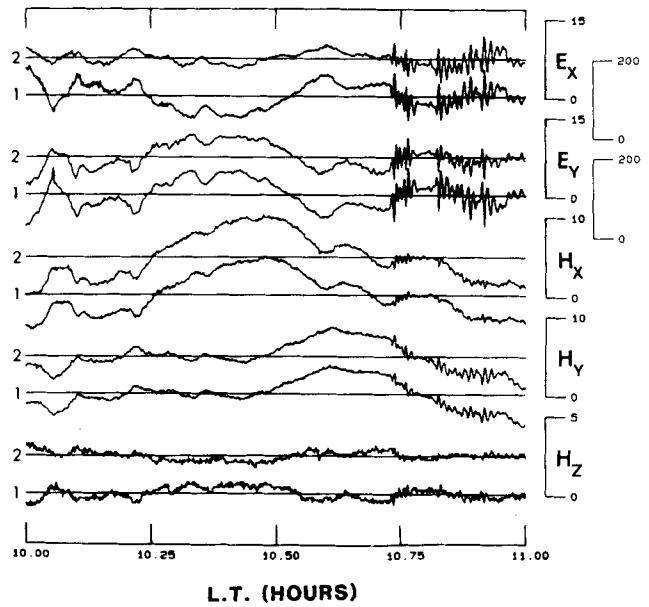

Figure 2. Example of 1 h of simultaneous data from sites 1 and 2. Note the different scales for the telluric components (E_x, E_y): the scale for site 1 is more than 13 times that for site 2. *E* field is in mV km^{-1} and *H* field is in nT.

SINGLE-SITE IMPEDANCE TENSOR ESTIMATION

In the general case of 2-D or 3-D geoelectric structure the MT impedance must be expressed by a second-rank tensor. At a particular frequency the tensor can be described by a linear system relating two horizontal magnetic components $\mathbf{H} = (H_x, H_y)$ as input with each of the electric field components $\mathbf{E} = (E_x, E_y)$ as output. The impedance tensor is defined in matrix notation as

$$\mathbf{E} = \mathbf{ZH} + \mathbf{E}_n, \tag{1}$$

where $\mathbf{E}$ and $\mathbf{H}$ represent the measured fields and $\mathbf{E}_n$ is the output noise. If frequency-band estimates are used it is assumed that $\mathbf{Z}$ changes slowly with respect to frequency within each band. Estimation of $\mathbf{Z}$ conventionally proceeds by least-squares reduction of the output-noise terms under the assumption that input-noise terms are negligible (Sims *et al.* 1971). A pair of components $\mathbf{F} = (F_x, F_y)$ is chosen to represent either $\mathbf{E}$ or $\mathbf{H}$ and equation (1) is multiplied by the complex conjugate $\mathbf{F}^*$ to provide dyadic matrix products of the field vectors. Estimates of $\mathbf{Z}$, referred to as $\hat{\mathbf{Z}}$, are obtained as

$$[\mathbf{EF}] = \hat{\mathbf{Z}}[\mathbf{HF}], \tag{2}$$

where [ ] represents a power spectral matrix. If $\mathbf{F} = \mathbf{H}$, then

$$\hat{\mathbf{Z}}^{\mathrm{d}} = [\mathbf{EH}][\mathbf{HH}]^{-1}, \tag{3}$$

which minimizes the error caused by noise in the output $\mathbf{E}$ and is referred to as a downward-biased estimate (superscript d).

Alternatively we may define an admittance tensor

$$\mathbf{H} = \mathbf{YE} + \mathbf{H}_n, \tag{4}$$

in which noise is assumed to reside only in the magnetic channels. As above the least-squares estimate of $\mathbf{Y}$ is

$$\hat{\mathbf{Y}} = [\mathbf{HE}][\mathbf{EE}]^{-1} \tag{5}$$

and this estimate minimizes error caused by noise in the output $\mathbf{H}$. We may relate impedance to an admittance as

$$\hat{\mathbf{Z}}^{\mathrm{u}} = \hat{\mathbf{Y}}^{-1}, \tag{6}$$

where the superscript u denotes an upward-biased estimate. Equations (3) and (6) provide two alternative estimates of the true impedance tensor $\mathbf{Z}$. Any attempt to assess the degree to which noise resides in either $\mathbf{E}$ or $\mathbf{H}$ is an ill-posed problem if only the above four fields are measured.

Although there are six least-squares solutions for each pair of impedance elements (Sims *et al.* 1971), all estimators contain measured auto-powers which are always biased estimates of the signal powers. If only the four basic fields are recorded, the measurements contain no redundancy with regard to the precise separation of signal and noise. All that can be achieved in practice is a bounded estimate in which the bounds are determined by the degree of bias. Here the downward biased estimate $\hat{\mathbf{Z}}^{\mathrm{d}}$ (3) and the upward biased

estimate $\hat{\mathbf{Z}}^u$ (6) are calculated in order to specify the bounds of the true impedance. Random errors, associated with each biased estimate, are calculated following the method described by Pedersen (1982).

Discussions of noise in relation to MT work can be found elsewhere (Kröger *et al.* 1983; Goubau *et al.* 1984; and Adám *et al.* 1986). The effect of bias errors on single-site MT impedance elements can be also found elsewhere (Sims *et al.* 1971; Hermance & Pedersen 1980; Cox *et al.* 1980).

The MT relationships can be expressed in a concise form if the field components are denoted by numbers. Here we adopt the convention: $H_x = 1$, $H_y = 2$, $E_x = 3$ and $E_y = 4$.

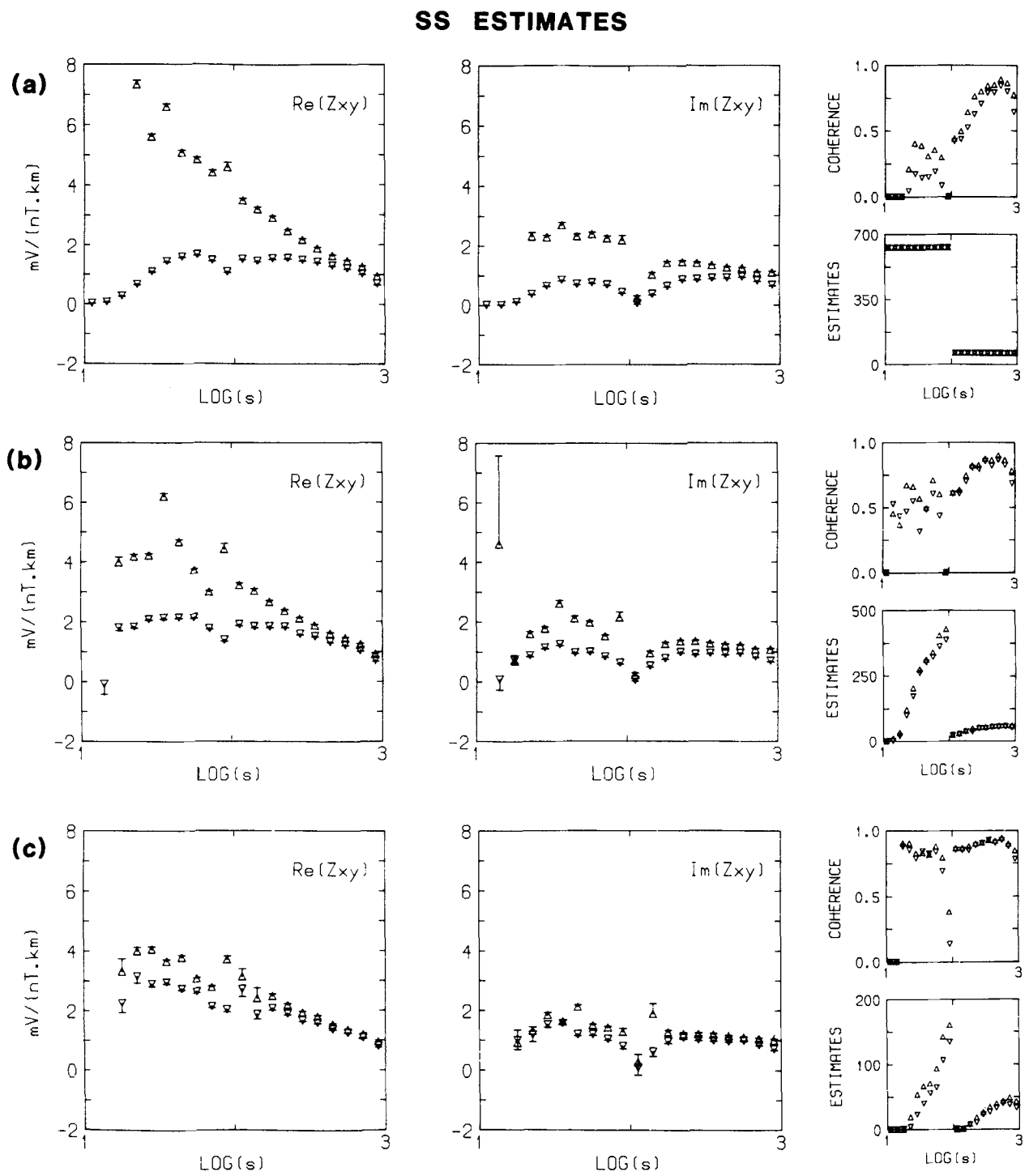

Figure 3. Single-site estimates of Z_{xy} using three different acceptance thresholds for the predicted coherence. (a) The threshold is 0.0, i.e. all data windows are accepted; (b) the threshold is 0.5 and in (c) it is 0.85. Both upward-(up-triangles) and downward-(down-triangles) biased cases are shown together with the associated 68 per cent random errors, shown as a single error bar for each bias case. For each row Re (Z_{xy}) is on the left and Im (Z_{xy}) is on the right. Far right shows the stacked predicted coherences (upper box) and number of estimates (lower box). Ordinates are linear and expressed in mV nT^{-1} km^{-1} while abscissae are expressed in logarithm of the period, *s*. Unless stated otherwise, all corresponding figures follow the same layout.

Spectral density functions can now be expressed as $S_{11} \leftrightarrow \overline{H_x H_x^*}$, for example. $\hat{\mathbf{Z}}$ will now denote a particular least-square estimate, $\hat{\mathbf{Z}}^{\mathrm{d}}$ or $\hat{\mathbf{Z}}^{\mathrm{u}}$, and $\boldsymbol{\eta}$ will denote an output noise term. In equation (1) there are two measured fields, **E** and **H**, which comprise unknown proportions of signal and noise and also an (unknown) output noise term. This last term conveys information on the combined noise in all the measurements. The predicted noise in all measurements is given by

$$\hat{\boldsymbol{\eta}} = \mathbf{E} - \hat{\mathbf{Z}}\mathbf{H} \tag{7}$$

and the predicted coherence is expressed as

$$\hat{\gamma}^2_{i12} = 1 - |\hat{\eta}_l|^2 / \hat{S}_{ii} \tag{8}$$

(Bendat & Piersol 1971) where $|\hat{\eta}_l|$ is the estimated noise autospectrum and $l = x, y$ when $i = 3, 4$. Depending on the choice of output, four predicted coherences can be estimated as $\hat{\gamma}^2_{312}$, $\hat{\gamma}^2_{412}$, $\hat{\gamma}^2_{134}$ and $\hat{\gamma}^2_{234}$. Other relevent coherence functions are the ordinary and partial coherence functions (Bendat & Piersol 1971). As all calculated coherence functions are biased estimates, we here use only unbiased expressions for the ordinary coherence (Carter *et al.* 1973) and for the predicted coherence (White 1973). This convention ensures that the partial coherences are also unbiased estimators.

The predicted coherence function (8) provides a measure of the noise power normalized with respect to the output power. It can be used to accept/eject estimates, or data realizations, associated with data windows containing noise at a certain normalized 'level'.

As noted in the introduction, we perform spectral stacking based on the noise content of individual data windows. Individual solutions for each frequency band are treated separately as indicated below. A selection procedure is required to reduce bias errors to acceptable levels. Fig. 3 illustrates the behaviour of the estimate bias when stacking at three levels of rejection using the predicted coherence function associated with each data window of the test data set. Results for the Z_{xy} element are shown in Fig. 3 using rejection levels of 0.0 (Fig. 3a), 0.5 (3b) and 0.85 (3c). The real and imaginary parts of Z_{xy} are shown as upward-($\hat{Z}^{\mathrm{u}}_{xy}$) and downward-($\hat{Z}^{\mathrm{d}}_{xy}$) biased curves together with their associated random errors. If $\hat{Z}^{\mathrm{u}}_{xy}$ and $\hat{r}^{\mathrm{u}}_{xy}$ are the upward-biased estimate and its corresponding random error and if $\hat{Z}^{\mathrm{d}}_{xy}$ and $\hat{r}^{\mathrm{d}}_{xy}$ are the equivalent downward-biased results, the results shown are

$$\hat{Z}^{\mathrm{u}}_{xy} + \hat{r}^{\mathrm{u}}_{xy} \quad \text{and} \quad \hat{Z}^{\mathrm{d}}_{xy} - \hat{r}^{\mathrm{d}}_{xy}.$$

The true, unknown, values usually lie somewhere between these two bounds. The results shown on the right are the final predicted coherences associated with the stacked results and the number of estimates, i.e. data windows, used in the stack. This method of presentation is repeated for all subsequent displays of impedance results. The need for a bias reduction scheme is evident in the results obtained. A consistent feature of our processing, which is displayed in the results of Fig. 3, is that the upward-biased solution displays a greater degree of bias offset than the equivalent downward-biased solution.

REJECTION TESTS FOR SPECTRAL STACKING

The most widely used acceptance criterion in MT uses only the predicted coherence and checks whether it is above a certain limit. Since a high value of the predicted coherence does not necessarily lead to reliable estimates, one may expect to refine this criterion using other coherence functions. For instance, input-coherent noise data may require setting an upper threshold for the ordinary coherence between input channels, in order to limit coupling effects (Pedersen & Svennekjaer 1984). Also, partial coherences may be used to ensure that the amount of coherent signal in the off-diagonal tensor elements is greater than the corresponding signal in the diagonal elements. This may be done by ensuring that the off-diagonal partial coherence is greater than that of the diagonal. A geometrical mean between predicted and off-diagonal partial coherence functions (Stanley & Frederick 1979) and also a phasor criterion (Word *et al.* 1970), where two geometrical means one for each output are combined together, are also considered.

Consider i and j as outputs, i.e. 3 and 4, and o and d as the off-diagonal and diagonal inputs respectively, e.g. 1 and 2. The five acceptance criteria, or tests, used are the following:

(1) $\hat{\gamma}^2_{ido} \geq \gamma^2_{\mathrm{t}}$
(2) $\hat{\gamma}^2_{ido} \geq \gamma^2_{\mathrm{t}}$ and $\hat{\gamma}^2_{io.d} > \hat{\gamma}^2_{id.o}$
(3) $\hat{\gamma}^2_{ido} \geq \gamma^2_{\mathrm{t}}$ and $\hat{\gamma}^2_{do} < \gamma^{12}_{\mathrm{t}}$
(4) $(\hat{\gamma}^2_{ido} \cdot \hat{\gamma}^2_{io.d})^{1/2} \geq \gamma^2_{\mathrm{t}}$
(5) $(\hat{\gamma}^2_{ido} \cdot \hat{\gamma}^2_{io.d} \cdot \hat{\gamma}^2_{jdo} \cdot \hat{\gamma}^2_{jo.d})^{1/4} \geq \gamma^2_{\mathrm{t}}$,

where γ^2_{t} and $\gamma^{1/2}_{\mathrm{t}}$ are thresholds for the predicted and ordinary coherences, respectively. Test (1) uses only the predicted coherence function ($\hat{\gamma}^2_{ido}$). Test (2) additionally requires that the off-diagonal partial coherence ($\hat{\gamma}^2_{io.d}$) is greater than the diagonal ($\hat{\gamma}^2_{id.o}$). Test (3) additionally requires that the input-field ordinary coherence ($\hat{\gamma}^2_{do}$ or $\hat{\gamma}^2_{od}$) is less than a certain level. Test (4) is a geometrical mean between predicted and off-diagonal partial coherences (Stanley & Frederick 1979). Test (5) is a phasor criterion (Word *et al.* 1970) in which two geometrical means, one for each output, are combined together.

For the data set considered a predicted threshold of $\gamma^2_{\mathrm{t}} = 0.85$ provides a good compromise between bias error levels and number of available estimates. A reasonable choice for the ordinary coherence threshold was found to be $\gamma^2_{\mathrm{t}} = 0.5$. It was found that tests 1, 2 and 4 produced the best results, where best is used in the sense of (a) reducing the bias, and (b) frequency stability of the impedance estimate, noting that the frequency bands are independent. Fig. 3 shows the results using test 1 for three different thresholds. Fig. 4 shows estimates of Z_{xy} obtained using tests 2 and 4 with a threshold $\gamma^2_{\mathrm{t}} = 0.85$. When test 4 is used, bias is reduced with respect to all other test results. It appears that this test does reject some 'inconsistent' data windows which other tests fail to detect. However, since this test is more stringent there are more bands with no acceptable results. Considering both real and imaginary parts, total error levels (i.e. bias and random) amount to 10 per cent on average for test 4. Differences in error levels among the three tests are equal to or less than 5 per cent for most of the bands.

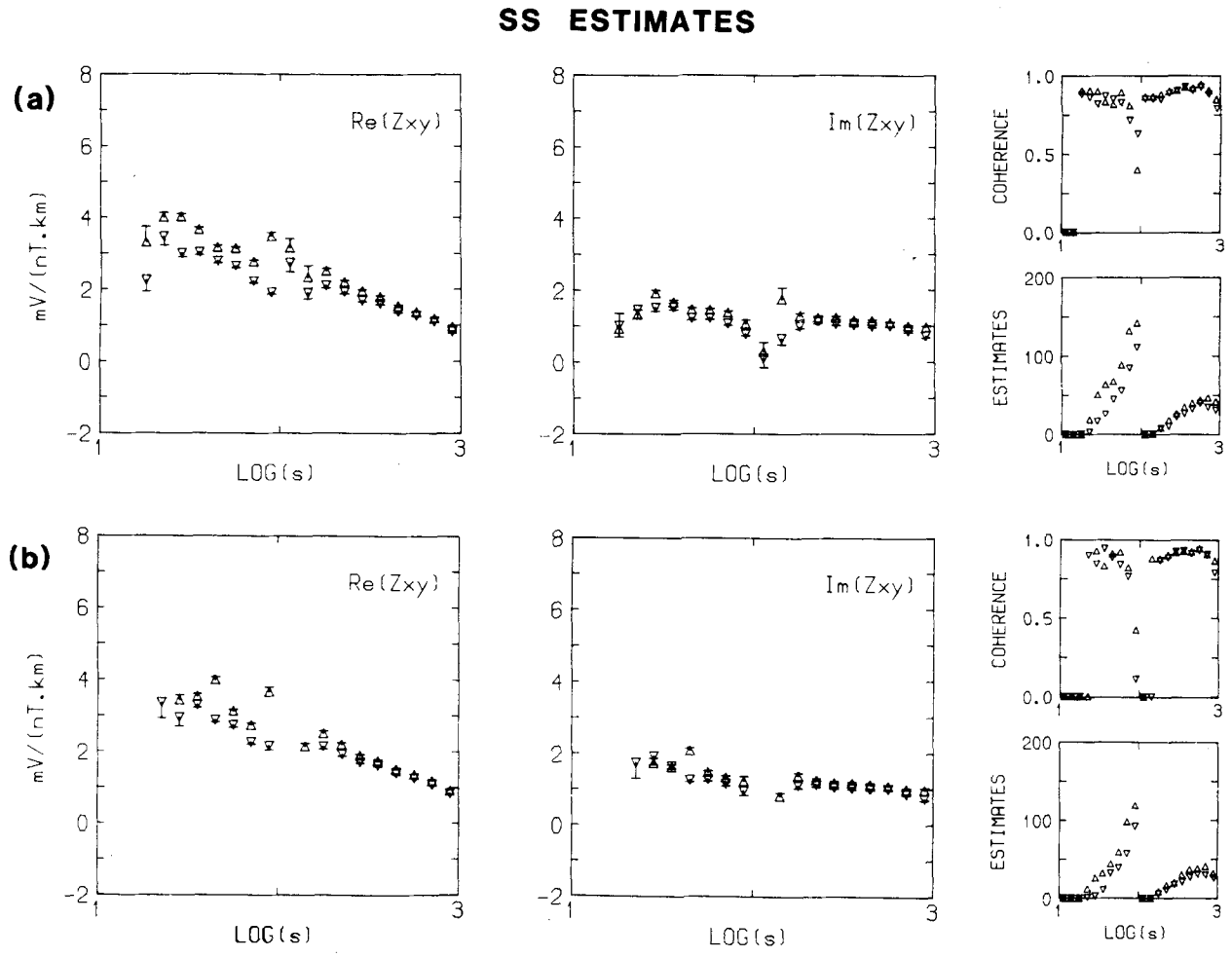

Figure 4. SS estimates of Z_{xy} using test 2(a) and test 4(b) with a threshold of 0.85.

Thus far we have not discussed how the two biased estimates can be combined to form a final SS estimate for each impedance element. Indeed this remains an unsolved problem as far as single-site MT estimation is concerned. As indicated by the results in Fig. 3 the problem cannot be precisely resolved since the degree of bias is unknown and differs between the $\hat{\mathbf{Z}}^u$ and $\hat{\mathbf{Z}}^d$ estimates. The results shown in Fig. 3 are typical in the sense that the upward-biased estimate consistently suffers a larger bias offset compared with the equivalent downward-biased estimate. Any averaging scheme as outlined by Beamish (1986) is never totally adequate. This is demonstrated for the same data set following a discussion on the remote reference technique. Only test 1 will be used for the remainder of this work.

REMOTE REFERENCE ANALYSIS

Since random errors tend to reduce when a sufficiently large data set is provided, bias errors eventually become the main source of uncertainty in single-site MT results. It is assumed here that bias arises predominantly from noise in the measured fields. An effective way of removing the bias errors in MT data analysis is given by the remote reference method (Goubau *et al.* 1978a,b). The RR estimate produces a bias-free estimate provided that noise at a reference (remote) site is incoherent with the noise at the local site. In practice this is accomplished by choosing a reference site at a sufficiently large distance from the base site. The degree of remoteness may vary from several kilometres to several metres (Goubau *et al.* 1984). Any precise definition of site separation would require a precise definition of noise sources.

The remote reference method requires measurement of two data channels at the remote site. Either the magnetic field or the electric field may be used as reference channels. it has been argued that since the electric field contains more noise and is prone to suffer from geoelectric polarization effects (Goubau *et al.* 1978a), one should usually use the magnetic field as a reference.

An important point worth mentioning is that, on account of the fact that two additional channel are measured, the variance of the RR estimates may be expected to be larger than that of the corresponding SS estimates (Kröger *et al.* 1983). However, according to the theoretical study by Stodt (1983), no significant inherent reduction in random error can be expected by using remote references in place of local references (SS estimation).

The impedance tensor is defined by (1). Assume a remote site where a horizontal field **R** is chosen. This field may be either a magnetic or an electric field. Assume that the noises in **R** are uncorrelated with the noises in both **E** and **H** at the base site. This assumption stems from the fact that the measured

fields are noisy and the response functions are expressed in terms of cross-spectral density functions.

Analogously to the downward-biased case of the single site estimate (3), a remote impedance tensor estimate is obtained by forming dyadic products with **R**, band-averaging and solving for **Z**

$$\hat{\mathbf{Z}}^R = [\mathbf{ER}][\mathbf{HR}]^{-1}, \tag{9}$$

where as before, [ ] denotes an average-power spectral matrix.

The variance in $\hat{\mathbf{Z}}^R$ can be estimated using an expression which resembles the one used for the SS analysis for some restricted situations (Pedersen 1982; Kröger *et al.* 1983). Here a more general expression for the variance is used. If the following assumptions are valid: (1) local noises are uncorrelated with **R**; (2) local noises are independent of signals; and (3) noises are stationary; the variance in $\hat{Z}_{ij}^R$ can be approximated by

$$\text{var}\,(\hat{Z}_{ij}^R) = \overline{|\hat{\eta}_i|^2}\;\overline{|A_j|^2}/(N\,|D|^2) \tag{10}$$

with an error of the order of $1/N$ (Gamble *et al.* 1979b). N is the number of degrees of freedom and

$$A_j = (-1)^{\delta_{jy}} R_x \cdot \overline{R_y H_k^*} + (-1)^{\delta_{jx}} R_y \cdot \overline{R_x H_k^*}, \tag{11}$$

where $i, j, k = x, y; k \neq j$. The δ_{jy}, δ_{jx} are Kronecker delta functions and $D = \det\{[\mathbf{HR}]\}$.

The above assumptions are likely to be satisfied in the case of a valid remote reference, i.e. the first assumption must be satisfied anyway. In addition, the analysis of Stodt (1983) suggests that (10) remains a valid approximation for the variance even when the local and reference field noises correlate. The second assumption is valid if noises are generated locally (note that if they are not, the first assumption would also fail). The stationarity of noise is required only in the sense that the ensemble average of the powers is equal to the measured time average (Gamble *et al.* 1979b). Since (10) is an approximation, there is a lower limit for N on which the error in the variance estimate is kept at a reasonable level.

The predicted coherence function is given by an expression similar to the one employed in the SS case (8). The RR value will be different from the SS estimate due to the explicit dependence on $\mathbf{Z}^R$. The RR predicted coherence function can be written as

$$\hat{\gamma}_{i12}^2 = 1 - |E_l - (\hat{Z}_{lx}^R H_x + \hat{Z}_{ly}^R H_y)|^2/\hat{S}_{ii}, \tag{12}$$

with $l = x, y$ when $i = 3, 4$. Other relevant coherence functions can also be expressed in terms of the RR impedance tensor. The predicted coherence given by (12) uses the local fields **E** and **H**. As the RR problem can be decomposed into a double least-squares problem (Jödicke & Grinat 1985), one could choose to use coherence functions for each problem separately. In the present work the predicted coherence given by (12) is used throughout. It not only gives the coherence between local fields but also is directly related to the combined local noise.

REMOTE REFERENCE RESULTS WITH R = H

It has been indicated that even low thresholds of the predicted coherence in remote reference analysis produce accurate impedance tensor estimates (e.g. Goubau *et al.* 1978a; Gamble *et al.* 1979a). If this is correct then coherence criteria such as the ones described in the last section are no longer important. The validity of this assertion is investigated here. Only test 1, i.e. the predicted coherence above a threshold, will be used as a selection criterion. Other tests are more restrictive, leading to more frequency bands with no estimates and a possible increase in the variance of the results.

The magnetic field components at site 1 are used as a remote reference. Fig. 5 shows the RR results for site 2 using a threshold of $\gamma_t^2 = 0.5$ (Fig. 5a), on the complete data sets of sites 1 and 2. The resulting predicted coherences are well above the threshold with the exception of only two bands. This result is, in some respects, the RR equivalent of the $\gamma_t^2 = 0.5$ SS results shown in Fig. 3(b). The suppression of bias is evident when SS and RR results are compared. Comparing the results of Figs 5(a) and 3(b), it is easy to see how bias degrades the accuracy of the SS estimates for most bands except those at long periods where coherences are high. This comparison demonstrates the power of the RR technique.

A more instructive comparison between RR and SS techniques is achieved using a higher threshold for the SS-predicted coherence function, since a threshold as low as $\gamma_t^2 = 0.5$ cannot produce SS results of acceptable accuracy. In order to compare SS and RR estimates we choose what could be called the best sets of estimates from both techniques. The SS results for a threshold $\gamma_t^2 = 0.85$ can be considered good in terms of bias errors, number of estimates available and variance levels. The RR results for a threshold $\gamma_t^2 = 0.5$ are chosen as the best set of RR estimates. The SS and RR results are shown in Figs 3(c) and 5(a), respectively. There are a few conclusions which can be drawn from these two figures. RR results are within the SS bounds for the majority of frequency bands and display a smoother behaviour. It can also be seen that RR estimates do *not* necessarily tend towards an arithmetic or even a weighted average of the two SS-biased estimates. We find that the RR error levels amount to 5 per cent for most bands and are always below the SS error levels.

Obviously, the choice of a particular threshold depends on the characteristics of the data set considered. It is in fact possible to use all the available data, i.e. with no coherence rejection, and still obtain reliable RR estimates for most of the bands. The RR results for this case are shown in Fig. 5(b). Estimates for the leftmost bands are not reliable and show large variances. Apart from these few frequency bands, the comparisons reveal that all available data can be used to provide reliable RR estimates. This feature will be investigated in more detail later. At the moment it is more instructive to concentrate on the behaviour of the variance estimated using the RR technique (10).

ON THE VARIANCE IN THE RR TECHNIQUE

The variance defined by (10) provides a quantitative way of assessing the quality of the impedance tensor estimates. The variance is inversely proportional to N, the number of degrees of freedom. The definition is only approximate and carries an error of the order of $1/N$ (Gamble *et al.* 1979b).

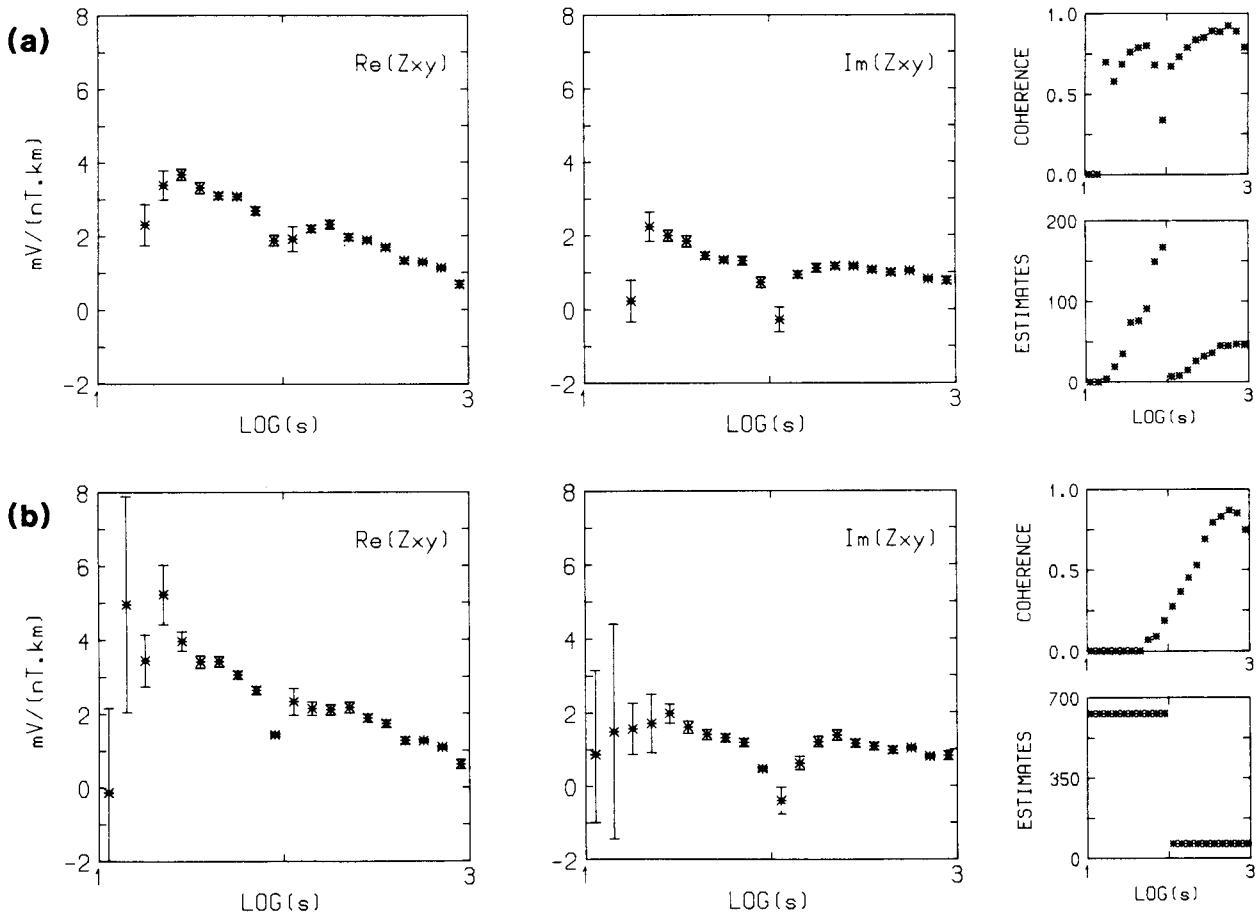

Figure 5. RR estimates of Z_{xy} using **H** as remote reference for two acceptance thresholds: 0.5(a) and 0.0(b). The error bars show the associated 68 per cent random errors.

In other words the variance is better approximated by (10) for $N \gg 1$, i.e. above a minimum value. Although the dependence on $1/N$ is not very strong, one may assume also that the variance can be progressively reduced by increasing N, the number of degrees of freedom. The more data that are collected and analysed, the smaller the variance should become. Although this idea is shared by several workers (e.g. Pedersen 1982; Kröger *et al.* 1983), it is not so straightforward since the variance is also a function of the error power, which in turn is simply related to the predicted coherence. There are still two other quantities in (10), A_j and D, which also contribute to the variance, but they do not depend on the local noise.

The investigation of how the estimated variance depends on the coherence and on N can be made using coherence sub-intervals and by fixing the number of degrees of freedom. We divide the coherence estimates available from the test data set into six distinct groups, numbered (i) to (vi).

(i) $= 0.0$ (ii) $(0.0, 0.25]$ (iii) $(0.25, 0.5]$
(iv) $(0.5, 0.75]$ (v) $(0.75, 0.9]$ (vi) $(0.9, 1.0]$.

Note that these sub-intervals are disjoint. We then choose N as the maximum available number of realizations it is possible to select for all sub-intervals. Due to the signal-to-noise characteristics of the test data set, this investigation is restricted to a few bands of decade 4.

It is possible to stack $N = 5$ realizations at all sub-intervals (i) to (vi) for band 5 of decade 4. This band is centered on 37.7 s. Fig. 6 shows the estimates of Z_{xy} for each of the six coherence sub-intervals. The estimate is indicated by its upper and lower 68 per cent confidence limits. The equivalent estimates obtained using the whole data set for the same frequency are indicated by the horizontal broken lines. We observe that the estimate for the last sub-interval (vi), obtained with $N = 5$ realizations, is identical to that obtained using the *whole data set* which contains $N = 630$ realizations. Increasing the confidence level to 95 per cent makes most of the six sub-intervals consistent with the estimates from the whole data set. A similar picture emerges when this last analysis is repeated for other frequency bands. Estimates from the last of the sub-intervals $(0.9, 1.0]$ agree with those computed using the whole data set with no data selection. Coherence selected estimates begin to differ from unselected estimates for $N \leq 4$.

These results indicate that the remote reference technique provides an inherent weighting which enhances the contribution of the higher-quality data. The accumulation of more data windows will not automatically reduce the

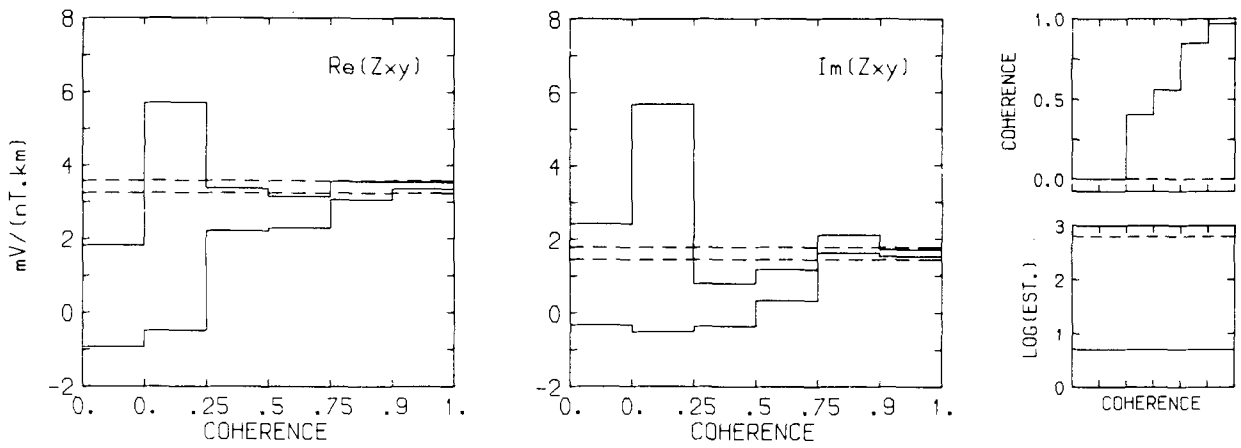

Figure 6. Remote reference estimates of Z_{xy} for band 5 of decade 4 using sub-intervals of predicted coherence (solid lines). The 6 sub-intervals are ordered from left to right as: = 0.0, (0.0, 0.25], (0.25, 0.5], (0.5, 0.75], (0.75, 0.9], and (0.9, 1]. The estimates are indicated by their upper and lower 68 per cent confidence limits. The number of degrees of freedom is fixed for all sub-intervals at $N = 5$. The broken lines show the estimates obtained for the same band, setting no coherence criterion, i.e. $N = 630$ estimates.

variance significantly. Accurate estimates are obtained using only data windows with low associated predicted error powers even for low values of N. In particular, only five realizations are sufficient to ensure results with better than 5 per cent accuracy. This indicates that the accuracy of remote reference estimates depends very little on data-set length but depends strongly on its *inherent noise content*. To be pragmatic, conventional SS estimation also benefits from this type of 'inherent weighting' as well, but only with regard to random errors. The results of Fig. 3(a) demonstrate the levels of *bias* introduced using SS estimation for the whole data set. The RR results of Figs 5 and 6 emphasize the performance of inherent weighting when 'true' signal autopowers are employed and bias is reduced.

The last two terms in the approximate definition of the variance (10) are $|A_j|$ and $|D|$, with A_j given by (11) and $D = \det\{[\mathbf{HR}]\}$ which depend only on the signals. We can extract the signal (subscript s) and noise (subscript n) terms in **H** and **R** to determine D as

$$D = \det\{[\mathbf{H_sR_s}] + [\mathbf{H_sR_n}] + [\mathbf{H_nR_s}] + [\mathbf{H_nR_n}]\}$$
$$= \det\{[\mathbf{H_sR_s}]\} = \det\{[\mathbf{H_sH_s}]\}.$$

In other words, D depends only on the signals since (1) remote noises are uncorrelated with local noises and (2) noises are independent of the signals. Moreover assuming that **R** is a magnetic field, D can be interpreted as the determinant of the coherence matrix of the magnetic field signals $[\mathbf{H_sH_s}]$. Polarization parameters can be obtained in terms of this matrix (Fowler *et al.* 1976). In particular, as $D \rightarrow 0$ the polarization of the signal **H** increases. Then at a certain noise level $|\hat{\eta}_i|^2$, the variance of $\mathbf{Z}^R$ diverges as the polarization of the signal increases. Obviously, the same conclusion applies to the estimate of the RR impedance tensor (9): as the polarization increases, the estimate also diverges. It is also easy to see that noise contributions to $|A_j|$ result in an additive term that, as long as noise powers in **R** can be considered sufficiently small, may be neglected. Thus $|A_j|$ can be approximated by its noise-free value.

REMOTE REFERENCE RESULTS WITH R = E

In principle the electric fields can be used as a remote reference. However, as electric channels are usually noisier than the magnetic ones, the variance should increase. Moreover the amplitude and hence the S/N of the electric components depends primarily on the local geoelectric structure (Goubau *et al.* 1978a), making them unsuitable as a remote reference. Fig. 7 shows the results obtained using **E** as a remote reference with a threshold of $\gamma_t^2 = 0.5$. It is clear that the estimate of **Z** obtained using **R** = **E** is subject to large uncertainties. These results can be compared with the equivalent **R** = **H** results shown in Fig. 5(a). The two results are not inconsistent; the estimates obtained using **R** = **E** are merely inaccurate. Note that the predicted error powers as monitored by the predicted coherences in Fig. 7 are similar to the corresponding coherences estimated using **R** = **H**, indicating that the *local* electric field is not particularly noisy.

The probable cause of the observed inaccuracy is the type of noise experienced by the reference **E** field used. A typical example of the noise affecting a significant number of **E** data windows at both sites is shown in Fig. 8. Both data and data first-differences are shown in this figure. The application of a straightforward first-difference formula is an effective high-pass filter with a gain of 2 at the Nyquist frequency. The first differences monitor the level shifts that occur within the sampling period. The **E** fields observed at both sites experienced severe level shifts. In the above example the shifts are not simultaneous, i.e. coherent, at the two sites. We observe however that the magnitude of a typical-level shift is far greater than the natural-signal level. In such circumstances, an adequate spectral representation of the data cannot be achieved since the power level at the Nyquist frequency is artificially large. When two data channels suffer this effect and are cross-correlated the results obtained will become unpredictable since both spectra are inadequate. Noise of the type shown in Fig. 8 was not

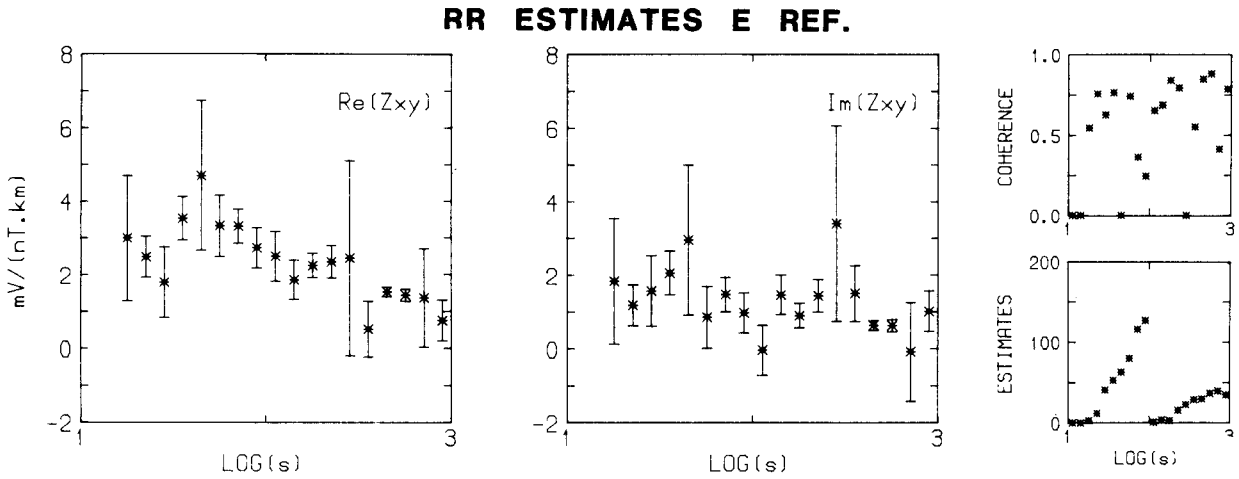

Figure 7. Remote reference estimates of Z_{xy} using **E** as a remote reference for a threshold 0.5.

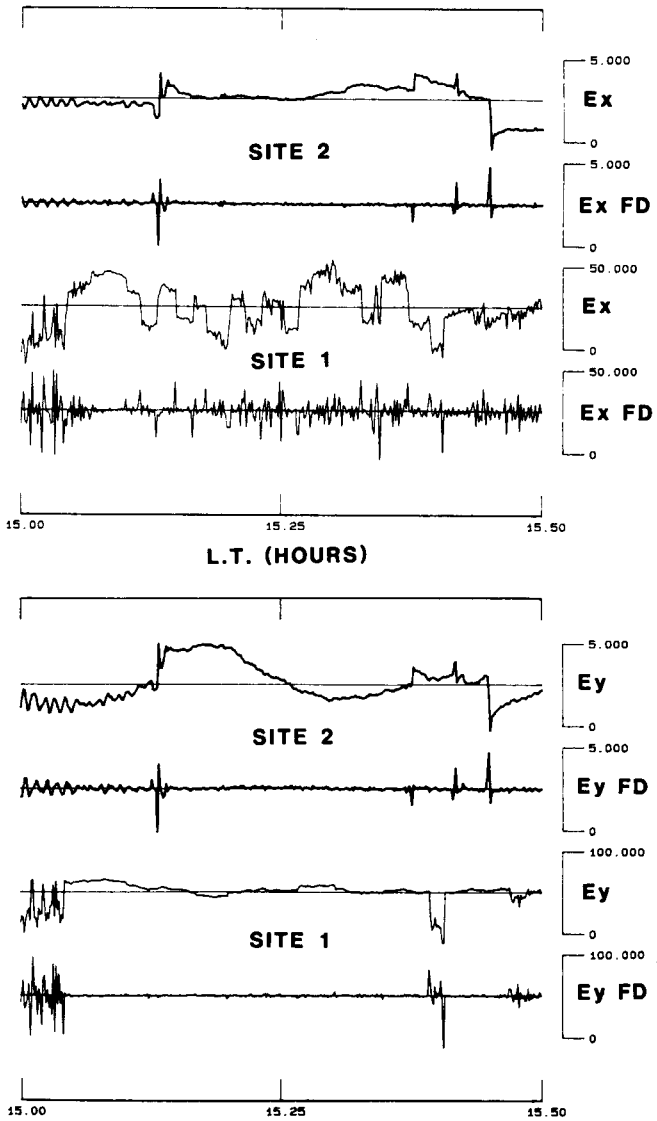

Figure 8. Electric field data recorded simultaneously for 30 min at sites 1 and 2. For each channel, first differences (FD) are plotted below the corresponding data. Upper frames show E_x and lower frames show E_y. Field units are in mV km^{-1} for data and mV km^{-1} Δt^{-1} for data first differences.

experienced in the magnetic fields at either of the two sites. We can say that when noise of the type considered here persists within a data set, strong limitations are imposed on the RR technique. Such limitations are due to an inadequate spectral representation caused by aliasing. It is generally true that such limitations are restricted to the **E** field (e.g. Adám *et al.* 1986).

THE ROLE OF THE PREDICTED COHERENCE

It has been shown that it is possible to obtain reliable RR estimates for most bands, using very low thresholds for the predicted coherences or even no selection at all. Nevertheless the accuracy of such estimates depends on their noise content. Since the RR technique provides an inherent weighting of the stacked realizations, it seems that just a few good signal-to-noise data windows are sufficient to produce good estimates. Obviously, if too few or no such data windows are available, the estimates will be inaccurate. The role of a selection criterion such as test 1, i.e. the predicted coherence, is to select adequate data windows. Although the predicted coherence was used with this objective in the SS analysis, its reliability is now greatly improved as a result of the robustness of the RR analysis. Good data windows are recognized and lower thresholds can be used, resulting in a more efficient use of the data set.

The results of Fig. 6 indicated that for a fixed number of degrees of freedom (N) the accuracy of the RR estimates is related to the signal-to-noise content of the local fields. That analysis was carried out at a single frequency. In order to emphasize how data windows with distinct noise levels contribute towards the final estimates, the exercise was repeated for the complete bandwidth. The degrees of freedom, N, or number of data windows, are now allowed to vary. The stacking of data windows with predicted coherences falling into the two bounded intervals (0.25, 0.5] and (0.7, 0.9] produced the two sets of results shown in Fig. 9. The data sets used in the two analyses are independent subsets of the test data set. While such a separation is artificial, the results demonstrate how the quality of a RR sounding is dependent on the local noise levels. These local noise levels can be monitored by the predicted coherence

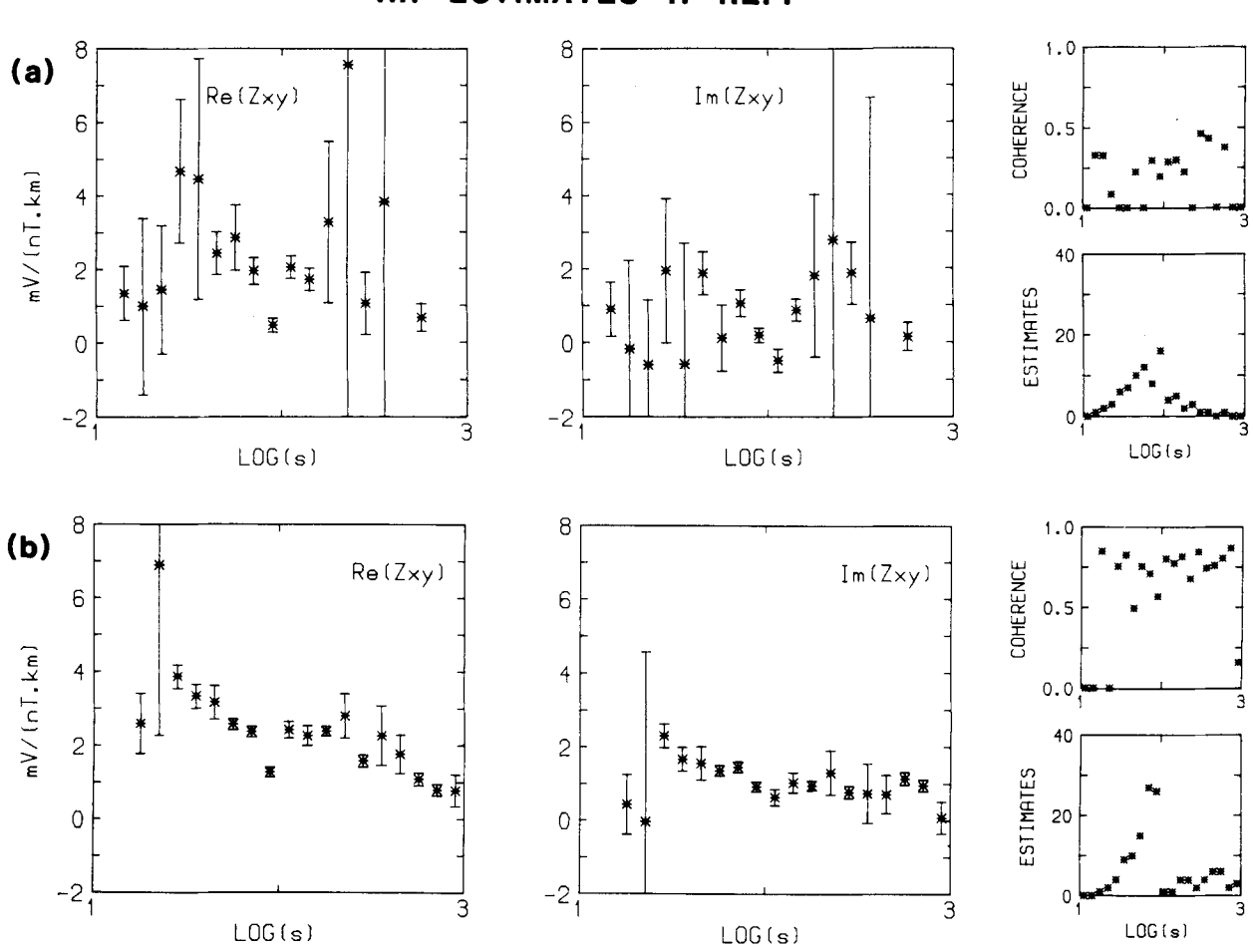

Figure 9. Remote reference estimates of Z_{xy} using **H** as a remote reference for two predicted coherence sub-intervals: (a) = (0.25, 0.5]; (b) = (0.7, 0.9].

function (8) and we suggest that this function has a significant role to play in the RR analysis.

The effectiveness of the RR-predicted coherence can be better understood by comparing it with its SS counterpart. It is necessary to change the notation in order to make the distinction between SS and RR coherences. We substitute the sub-indices of $\hat{\gamma}^2_{ijk}$ by either L, when dealing with downward-biased SS estimates (8), or by either RH or RE (12), when referring to RR estimates. RH will be used for a result involving the remote magnetic field while RE will be used for a result involving the remote electric field. Under this notation, $\hat{\gamma}^2_{312}$ and $\hat{\gamma}^2_{412}$ will be written as $\hat{\gamma}^2_L$ for the SS case, or as either $\hat{\gamma}^2_{RH}$ or $\hat{\gamma}^2_{RE}$ when H or E is used as a remote reference, respectively.

Comparisons between SS- and RR-predicted coherences indicate that the downward-biased SS estimate of the predicted coherence is always greater than or equal to its RR equivalent, irrespective of the remote channel, i.e.

$$\hat{\gamma}^2_L \geq \hat{\gamma}^2_{(RH;RE)}. \tag{13}$$

As this empirical result holds true for all bands, band 3 of decade 4, centred on 56.6 s, is chosen as an example. Fig. 10 shows the estimates of $\hat{\gamma}^2_L$ plotted against $\hat{\gamma}^2_{RH}$, considering both E_x and E_y as the outputs and using all 630 data windows of the test data set.

In Fig. 10 there are many points where only $\hat{\gamma}^2_{RH}$ is zero. It is worth examining these points since they shed more light on the question of how effective RR- and SS-predicted coherences are in recognizing noisier realizations. The equality limit of relation (14) is indicated by the equivalence diagonal in Fig. 10. Apart from the exactitude of the inequality, we note that as $\hat{\gamma}^2_L \rightarrow 0$ then $\hat{\gamma}^2_{RH} \rightarrow 0$ much more rapidly. Basically, the SS analysis consistently indicates higher signal-to-noise levels than its RR counterpart. The fact that such high levels are false and are an artifact of coherent local noise is demonstrated by the horizontal distribution of points where $\hat{\gamma}^2_{RH} = 0$. Quite clearly the test data set contains a large number of realizations with high local SS coherence values which correspond to a null RR coherence. The introduction of additional information through the reference channels enables such inadequate data windows to be identified and rejected. The results that emerge when the electric field is used as a reference are very similar to those of Fig. 10. We conclude that the RR-predicted coherence obtained using the remote electric field is a reliable measure of the noise content of our local fields.

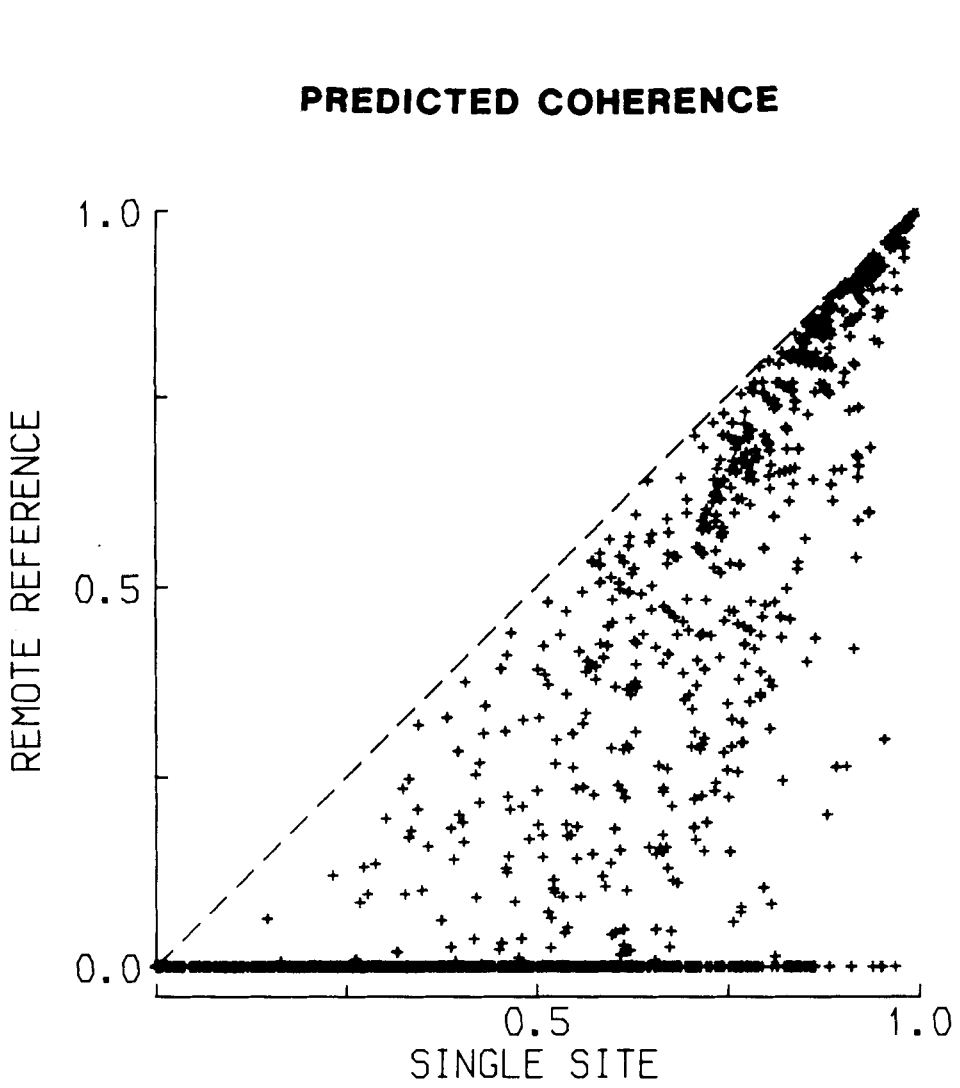

Figure 10. Plot of remote-reference predicted coherence against single-site predicted coherence for band 3, decade 4 using both E_x and E_y as outputs. The number of estimates is 2×630. The dashed line is the equivalence line of the two coherences.

COHERENCE SELECTRION OF DATA SUBSETS AND A HYBRID TECHNIQUE

It is worth stressing that relation (13) holds irrespective of the choice of the remote fields. This suggests that $\hat{\gamma}^2_{RH}$ and $\hat{\gamma}^2_{RE}$ are both of comparable efficiency in selecting adequate data sets, with respect to their noise content. The composition of data subsets selected by using either *RH* or *RE* and setting several thresholds for the predicted coherences in the range [0, 1] was investigated. The comparison of impedance tensor estimates using *RH*- and *RE*-derived data subsets brings new facts to light. Test 1 with a threshold of $\gamma^2_t = 0.5$ is still used as an acceptance criterion in order to illustrate the results. Only the magnetic field is used as a remote reference for the final estimate of $\mathbf{Z}$, but both $\hat{\gamma}^2_{RH}$ and $\hat{\gamma}^2_{RE}$ are calculated and then used in the selection of data subsets. Three data subsets can be selected: an *RH*-derived, an *RE*-derived and an *RHE*-derived data subset. The last subset contains the realizations which belong to both previous subsets. It is worth remembering that $\hat{\gamma}^2_{RH}$ is used to select the first data subset, while $\hat{\gamma}^2_{RE}$ is used to select the second one. In all cases analysed the *RH*-derived subset is larger than the *RE*-derived subset, the difference between them being relatively greater for decade 5. Data belonging to the intersection of the two data sets account for most of the accepted realizations. The realizations in the intersection of the *RH*- and *RE*-derived data sets contribute 71 per cent, or more, of all the accepted realizations.

Only *RH*- and *RE*-derived data subsets will be used to illustrate the results. Fig. 11 shows the estimates for the off-diagonal element Z_{xy}, using *RH*- and *RE*-derived data subsets. Both sets of estimates exhibit similar values and, apart from bands where there are few realizations, both estimates agree well. The two sets of estimates are comparable using criteria such as smoothness, variance level and predicted coherence. Similar results are obtained when comparing *RH*- and *RHE*-derived subsets, although *RHE*-derived predicted coherences are higher than their *RH*-counterparts.

Although remote reference estimates are poor when a remote electric field is used, the above results suggest that the predicted coherence obtained is still effective in detecting noise present in the measured powers. Its utility lies in data-windowing or rejection, yielding cleaner data sets. This can be shown using the single-site least-squares

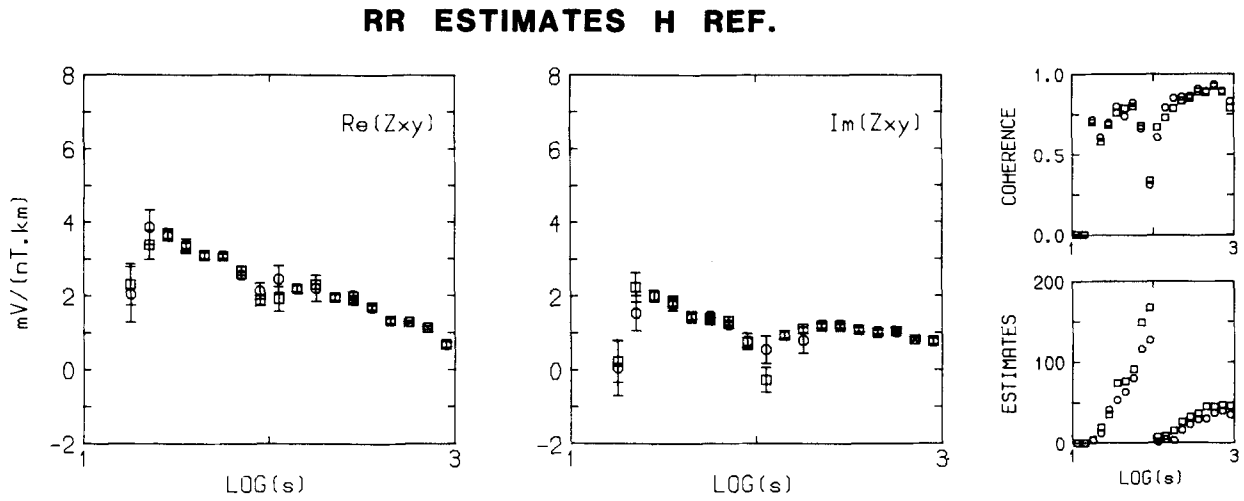

Figure 11. Remote reference estimates of Z_{xy} from *RH*-selected (squares) and *RE*-selected (circles) data subsets. Acceptance threshold is 0.5.

framework on RR selected data subsets. The motivation behind it lies in the expectation that bias errors will be reduced as a result of the lower noise levels present in the selected subsets. As this reduction should be achieved irrespective of the remote channels, it is more interesting to restrict this investigation to the *RE*-selected data subset, i.e. the subset obtained using $\mathbf{R} = \mathbf{E}$. Estimates of $\mathbf{Z}$ are then obtained through SS analysis of the selected subset.

We use $(\gamma_t^2)_{RE} = 0.5$ as a threshold for the RR-derived predicted coherence $\hat{\gamma}_{RE}^2$. Relation (13) shows that any threshold $(\gamma_t^2)_L \geq 0.5$ may be chosen for the SS-derived predicted coherences. Fig. 12 shows the SS estimates of Z_{xy} using a threshold $(\gamma_t^2)_L = 0.5$. A reduction in the bias error is evident when these subset estimates are compared with the earlier and equivalent SS results shown in Fig. 3(b). The estimates obtained from this hybrid scheme are comparable to SS results selected at much higher thresholds. The difference lies in the fact that data windows come from data subsets already selected in terms of their signal content using the RR technique. It is important to remember that it is not advisable to set a higher threshold for $\hat{\gamma}_{RE}^2$ since the number of the accepted realizations drops significantly. The same conclusions are obtained from *RH*-selected data subsets. In fact *RE*- and *RH*-selected data subsets produce similar SS results.

One may ask the usefulness of using a remote electric reference for selecting data sets since, in the end, a SS framework is used to estimate $\mathbf{Z}$. Such a hybrid technique might prove useful in situations where for any reason, e.g. economic, it is not possible to record remote magnetic channels, but remote electric channels are feasible. Accurate RR estimates of $\mathbf{Z}$ may prove difficult to obtain using a remote electric field. As the data subset obtained using this hybrid technique contains only low noise level realizations, it is possible to obtain less-biased SS estimates of $\mathbf{Z}$ than would otherwise be possible. In addition it should be possible to use the electric information from the remote telluric site as well (Hermance & Thayer 1975). Results

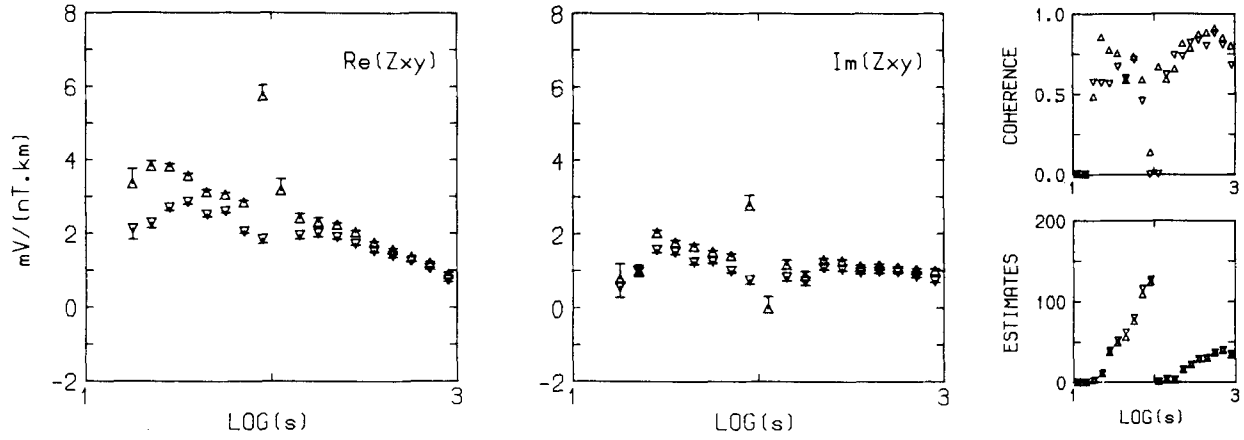

Figure 12. Estimates of Z_{xy} using SS technique on *RE*-derived data sets for a remote acceptance threshold of 0.5. Both upward-biased (up-triangles) and downward biased (down-triangles) are shown together with their associated 68 per cent random errors. Local threshold is 0.5.

obtained from the hybrid scheme are intermediate and lie between the usual SS results and those obtained from a RR analysis using a remote magnetic field.

SUMMARY

This case study has used a typical MT data set collected at two sites. It has considered several processing methods that can be used to provide accurate determinations of the impedance function. Throughout the study we have used coherence-based selection of data windows containing adequate solutions. The term 'adequate' is used in the sense that the distribution of solutions obtained should obey Gaussian-type statistics with no outliers. If the selection procedure can be termed adequate then simple spectral stacking of individual solutions works well and there is no need to resort to a statistically more robust treatment such as that described by Egbert & Booker (1986). A comparison of the coherence functions obtained from SS and RR methods has, however, revealed that in many cases the SS-predicted coherence must be viewed as an 'inadequate' selection criterion.

It has been demonstrated that bias errors eventually become the main source of uncertainty in SS magnetotelluric results. All that can be achieved in practice is a bounded estimate in which the bounds are determined by the degree of bias. The degree of bias is a function of the S/N within the data set and is always likely to be a function of frequency. In order to arrive at a final SS estimate, at least two biased estimates must be combined. We have demonstrated, by comparing SS and RR results, that no combining procedure can ever be totally adequate since the degree of bias remains undefined for the SS case. In our opinion an inadequate combining procedure can produce a false, bias-dependent gradient into the SS impedance function.

We have investigated a number of coherence-based selection schemes that can be applied to the SS case. The most effective and practical procedure always involves the predicted coherence function. For our data the best set of results was obtained using a geometrical mean between the predicted and off-diagonal partial coherences (Stanley & Frederick 1979). Total error levels in the off-diagonal impedance elements amount to 10 per cent on average for the SS case.

The RR technique allows the determination of unbiased estimates of the impedance function. The RR error levels amount to 5 per cent as a typical average over frequency, for our data set. The suppression of bias errors in the RR results allows all the data to be used in the estimation procedure. However, our results reveal that although the RR technique provides an inherent weighting which enhances the contribution of the higher-quality data, the accuracy of the results still depends on the signal levels. The accumulation of more data will not automatically reduce the variance level of the impedance function. Our results demonstrate that the variance of a RR estimate is strongly dependent on the local S/N ratio. This ratio can be readily monitored by the RR equivalent of the predicted coherence function used for data selection in the SS case.

The RR impedance estimates obtained using the reference electric field were inaccurate. This is because of the presence of persistent noise in the two reference electric channels. Despite being incoherent, such reference field noise imposes strong limitations on the RR technique. We note, however, that despite the severity of the noise the resulting RR estimates are not inconsistent, but merely inaccurate. The comparisons between the SS- and the RR-predicted coherence functions showed the reliability of the latter in selecting adequate data windows. Moreover, comparisons between RR-predicted coherence functions indicate that the predicted coherence obtained using the reference electric field is a reliable measure of the noise content of our *local* fields. In such circumstances the RR-predicted coherence can be used for adequate data selection although the corresponding impedance estimates are not accurate. In situations where only a reference electric field can be afforded we suggest a hybrid technique that may prove to be useful. The RR-predicted coherence can be used to overcome the problem of inadequate data selection. The selected data windows can then be processed by the SS method to provide a less-biased, although still bounded, impedance function.

ACKNOWLEDGMENTS

The data collection was supported by the National Environment Research Council, the Overseas Development Administration and Kandilli Observatory, Bogazici University. The TDP3 experiment also received support and encouragement from the Technical University of Istanbul. The authors thank reviewers and the Associate Editor for comments. This paper is published with the permission of the Director, British Geological Survey (NERC). One of the authors (JMT) acknowledges the award of a research studentship from the Brazilian Research Council (CNPq).

REFERENCES

Adám, A., Szarka, L., Verö, J., Wallner, A. & Gutdeutsch, R., 1986. Magnetotellurics (MT) in mountains—noise, topography and crustal inhomogeneity effects, *Phys. Earth planet. Int.*, **42,** 165–177.

Beamish, D. & Riddick, J. C., 1985a. TDP3 I. Background to the project, *GRG Report 85/21, British Geological Survey.*

Beamish, D. & Riddick, J. C., 1985b. TDP3 II. Magnetotelluric array instrumentation, *GRG Report 85/22, British Geological Survey.*

Beamish, D., 1986. Deep crustal geoelectric structure beneath the Northumberland Basin, *Geophys. J.R. astr. Soc.*, **84,** 619–640.

Bendat, J. S. & Piersol, A. G., 1971. *Random Data: Analysis and Measurement Procedures,* Wiley-Interscience, New York.

Carter, G. C., Knapp, C. H. & Nuttal, A. H., 1973. Estimation of the magnitude-squared coherence function via overlapped Fast Fourier Transform Processing, *IEEE Trans. Audio Electroacoust., AU-21,* **4,** 337–344.

Cox, C. S., Filloux, J. H., Gough, D. I., Larsen, J. C., Poehls, K. A., von Herzen, R. P. & Winter, R., 1980. Atlantic lithosphere sounding, in *Advances in Earth and Planetary Sciences,* vol. 9, pp. 13–32, ed. Schmucker, U., Center for Academic Publications, Tokyo.

Egbert, G. D. & Booker, J. R., 1986. Robust estimation of geomagnetic transfer functions, *Geophys. J.R. astr. Soc.*, **87,** 173–194.

Evans, R., Beamish, D., Crampin, S. & Üçer, S. B., 1987. The Turkish Dilatancy Project (TDP3): multidisciplinary studies of a potential earthquake source region, *Geophys. J.R. astr. Soc.*, **91,** 265–286.

Fowler, R. A., Kotick, B. J. & Elliott, R. D., 1967. Polarization

analysis of natural and artificially induced geomagnetic micropulsations, *J. geophys. Res.*, **72,** 2871–2883.

Gamble, T. D., Goubau, W. M. & Clarke, J., 1979a. Magnetotellurics with a remote reference, *Geophysics,* **44,** 53–68.

Gamble, T. D., Goubau, W. M. & Clarke, J., 1979b. Error analysis for remote magnetotellurics, *Geophysics,* **44,** 959–968.

Goubau, W. M., Gamble, T. D. & Clarke, J., 1978a. Magnetotellurics using lock-in signal detection, *Geophys. res. Lett.*, **5,** 543–546.

Goubau, W. M., Gamble, T. D. & Clarke, J., 1978b. Magnetotelluric data analysis: removal of bias, *Geophysics,* **43,** 1157–1166.

Goubau, W. M., Maxton, P. M., Koch, R. H. & Clarke, J., 1984. Noise correlation lengths in remote reference magnetotellurics, *Geophysics,* **49,** 433–438.

Gundel, A., 1977. Estimation of transfer functions with reduced bias in geomagnetic induction studies, *Acta Geodaet., Geophys. Montanist. Acad. Sci. Hung.*, **12,** 345–352.

Hermance, J. F. & Thayer, R. E., 1975. The telluric-magnetotelluric method, *Geophysics,* **40,** 664–668.

Hermance, J. F. & Pedersen, J., 1980. Deep structure of the Rio Grande rift: a magnetotelluric interpretation, *J. geophys. Res.*, **85,** 3899–3912.

Jödicke, H. & Grinat, M., 1985. Magnetotelluric measurements at the SE flank of the Stavelot-Venn anticline using the remote reference technique, *N. Jb. Geol. Paläont. Abh.*, **171,** 425–440.

Kröger, P., Michel, H. J. & Elsner, R., 1983. Comparison of errors in local and reference estimates of the magnetotelluric impedance tensor, *J. geophys.*, **52,** 97–105.

Larsen, J. C., 1980. Electromagnetic response functions from interrupted and noisy data, *J. Geomag. Geoelect.*, **32,** Suppl. I, 89–103.

Park, J. & Chave, A. D., 1984. On the estimation of magnetotelluric response functions using the singular value decomposition, *Geophys. J.R. astr. Soc.*, **77,** 683–709.

Pedersen, L. B., 1982. The magnetotelluric impedance tensor—its random and bias errors, *Geophys. Prospect.*, **30,** 188–210.

Pedersen, L. B. & Svennekjaer, M., 1984. Extremal bias coupling in magnetotellurics, *Geophysics,* **49,** 1968–1978.

Sims, W. E., Bostick Jr., F. X. & Smith, H. W., 1971. The estimation of magnetotelluric impedance tensor elements from measured data, *Geophysics,* **36,** 938–942.

Stanley, W. D. & Frederick, N. V., 1979. U.S. Geological Survey real-time MT system, *USGS Open File 79–R27.*

Stodt, J. A., 1983. Noise analysis for conventional and remote reference magnetotelluric data, *PhD dissertation,* University of Utah.

White, R. E., 1973. The estimation of signal spectra and related quantities by means of the multiple coherence function, *Geophys. Prosp.*, **21,** 660–703.

Word, D. R., Smith, H. W. & Bostick Jr., F. X., 1970. An investigation of the magnetotelluric tensor method, *Elect. Geophys. Res. Lab. Tech. Rep.*, **82,** The Univ. Texas at Austin, Austin.